doi: 10.13133/2280-6148/18133 *Journal of Mediterranean Earth Sciences 15 (2023), xx-xx*

J M E S **Journal of Mediterranean Earth Sciences**

New insights on the fossil mammals from Casal de'Pazzi (Rome)

Luca Pandolfi [1,*], Roberta Martino [2], Maria Rita Palombo [3]

[1] *Dipartimento di Scienze, Università della Basilicata, Potenza, Italy*
[2] *Department of Earth Sciences, GeoBioTec, NOVA School of Science and Technology, Universidade NOVA de Lisboa, Caparica, Portugal*
[3] *CNR- IGAG, Istituto di Geologia Ambientale e Geoingegneria, Area della Ricerca di Roma 1, Roma, Italy*
** Corresponding Author: luca.pandolfi@unibas.it*

ABSTRACT - The mammal fauna from Casal de'Pazzi (Rome) has been listed in several papers during the past decades, but a detailed taxonomic study has never been published. In this paper, the specimens retrieved or still embedded in sediments from the musealized area of the Casal de'Pazzi site are described and compared for the first time. The morphological and morphometric analyses allow the detection of the following taxa: *Palaeoloxodon antiquus*, *Canis* cf. *lupus*, *Crocuta* cf. *spelaea*, *Equus* sp., *Stephanorhinus kirchbergensis*, *Hippopotamus* cf. *amphibius*, *Sus scrofa*, *Cervus elaphus*, *Dama dama,* and *Bos primigenius*. The studied remains, although comprising a small sample compared to those collected in situ during excavations, represent an important record in the context of the Middle Pleistocene faunal assemblages of the Roman Basin.

Keywords: taxonomy, morphology; morphometry; mammalian fauna; Middle Pleistocene; Central Italy.

Submitted: 28 June 2023 -Accepted: 24 August 2023

1. INTRODUCTION

The site of Rebibbia-Casal de' Pazzi is located in the lower Aniene river valley within the suburban area of Rome. The archeological excavations were carried out between 1981 and 1986, yielding over 2000 faunal remains. Anzidei et al. (1984) published a preliminary list of mammal taxa collected from the site, which includes *Elephas (Palaeoloxodon) antiquus*, *Bos primigenius*, *Cervus elaphus*, and *Equus ferus*. The faunal assemblage was correlated with other late Middle Pleistocene assemblages collected from the Roman area, such as Torre in Pietra (upper levels) and Vitinia (upper levels), chronologically referred to MIS 7 (Caloi et al., 1998; Palombo et al., 2003; Marra et al., 2017, 2018; Petronio et al., 2019). Palombo et al. (2003) partially amended the mammal fauna reported by Anzidei et al. (1984, 1999) on the basis of a partial examination of large mammal remains and listed the following taxa: ? *Canis* sp. aff. *C. arnensis*, *Canis lupus*, *Crocuta crocuta*, *Elephas (Palaeoloxodon) antiquus*, *Equus ferus*, *Stephanorhinus* sp., *Sus scrofa*, *Hippopotamus* ex gr. *amphibius*, *Capreolus capreolus*, *Dama dama tiberina*, *Cervus elaphus,* and *Bos primigenius*. The faunal list published by Palombo et al. (2003) was then reviewed by Kotsakis and Barisone (2008) that included *Canis* sp. instead of ? *Canis* sp. aff. *C. arnensis*, and by Marra et al. (2017) with minor changes, i.e., *Palaeoloxodon antiquus*, *Hippopotamus* cf. *amphibius*, *Cervus elaphus* ssp., *Dama dama* ssp.

However, despite being cited in several papers (e.g., Segre, 1983; Anzidei and Gioia, 1990; Manzi et al., 1990; Anzidei et al., 2004; Kotsakis and Barisone, 2008; Gioia, 2004; Gioia and Peresani, 2011), the mammal fauna from Casal de'Pazzi (CdP) has never been studied or revised in detail. The aim of this contribution is to describe and compare the large mammal remains either retrieved or still embedded in sediments of the CdP musealized area and to provide their compelling taxonomic classification.

The taxa biochronological framework and a few paleoecological information are given in a separate paper included in this special issue (i.e., Palombo, 2023, this volume).

2. MATERIAL STUDIED AND METHODS

The material here described is currently housed at the Museum of Casal de'Pazzi (MCP) and represents a selection of the specimens collected during the excavation of the site. The majority of the material retrieved from the deposit is stored at the Soprintendenza Speciale Archeologia Belle Arti e Paesaggio di Roma, and it is currently not available.

According to the terminology herein adopted, upper-case letters and lower-case letters, respectively, indicate upper and lower premolars and molars (i.e., P/p and M/m, respectively). Upper and lower deciduous teeth are indicated as Dp and dp respectively.

Concerning Proboscidean, the term "platelet" is adopted to indicate the small element, which, conversely to talon (x), does not fuse together with the last plate but extends to the crown base on the proximal side of the last molars (M3/m3) (Lister and van Essen, 2003). Premolar and molar specimens were measured with a digital caliper following Aguirre (1969), Maglio (1973), and Lister (1996a), except for the lamellar frequency that has been calculated by averaging the values taken on the occlusal surface and labial and lingual sides. In moderately worn teeth, the putative missing plates have been inferred detecting the presence of the large first root (Sher and Garutt, 1987). According to Albayrak and Lister (2012), upper and lower last molars in British *P. antiquus* generally display from one to two or three plates converging to the first root. Our personal observations roughly support these results.

Canidae and Hyaenidae remains were measured following Boudadi-Maligne (2010) and Lewis and Werdelin (2022), respectively.

Morphological nomenclature of Rhinocerotidae teeth follows Antoine (2002), Lacombat (2005), and Fortelius et al. (1993).

The morphological terminology for the hippopotamid material follows Boisserie et al. (2010) and Mazza (1995). All the remains were measured following the protocols reported in Caloi et al. (1980) and Mazza (1995). A supplementary comparative table is provided as table S1 (supplementary material, compiled data from Hooijer, 1950; Accordi, 1955; Harris, 1991; Mazza, 1991, 1995; Galobart et al., 2003; Mazza and Bertini, 2013; and direct observations).

Morphological and morphometric features used to describe and discriminate Cervidae and Bovidae follow, among others, Brugal (1985), Sala (1986), Gee (1993), Di Stefano (1995), and Lister (1996b). Dental and postcranial remains were measured following Driesch (1976) and include the maximal length (L), the distal transverse diameter (DTD), the distal antero-posterior diameter (DAPD), the transverse diameter of the shaft (TDS), the lateral height (Hlat), the medial height (Hmed), and the antero-posterior diameter measured on the medial face (APDM).

3. SYSTEMATIC PALEONTOLOGY

Class Mammalia Linnaeus, 1758
Order Proboscidea Illiger, 1811
Superfamily Elephantoidea Gray, 1821
Family Elephantidae Gray, 1821
Subfamily Elephantinae Gray, 1821
Tribe Elephantini Gray, 1821
Genus *Palaeoloxodon* Matsumoto 1924
Palaeoloxodon antiquus (Falconer and Cautley, 1847), Figs. 1 and 2, Tab. 1

Material: The straight-tusked elephant remains, either retrieved or still embedded in sediments of the CdP musealized deposit, consist of 29 specimens (i.e., 2 cranial fragments, cranium and mandible; 9 almost complete tusks plus 15 tusk fragments; 9 variously preserved teeth, 2 premolars and 7 molars, plus 5 badly preserved tooth fragments; 3 incomplete limb bones, scapula, humerus,

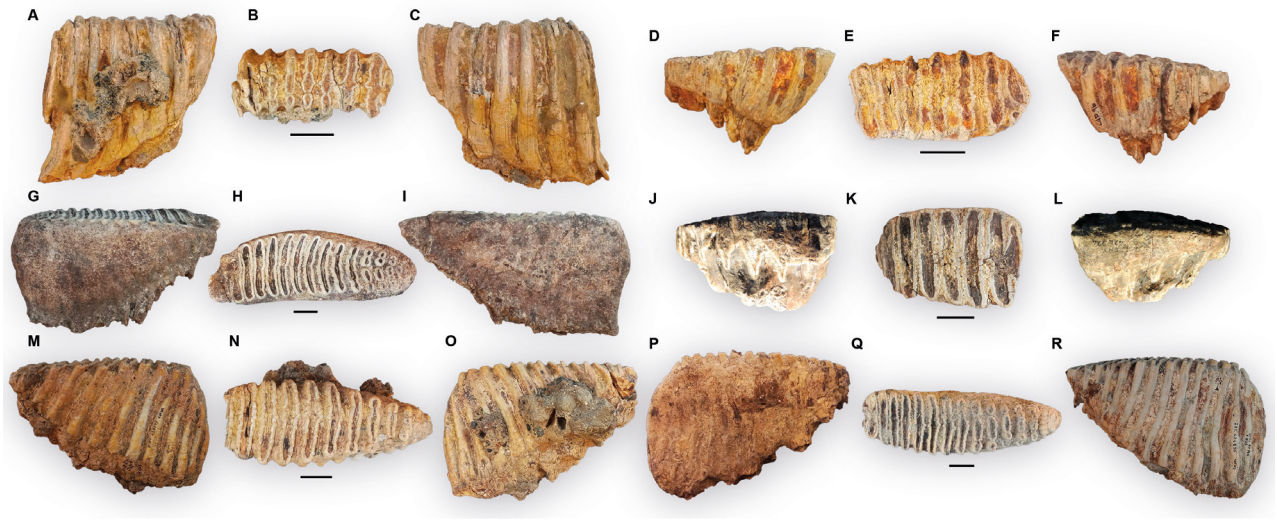

Fig. 1 - *Palaeoloxodon antiquus* upper teeth from Casal de'Pazzi. (A-C) CdP95 right Dp4, in A) labial view, B) occlusal view, and C) lingual view; (D-F) CdP96 right Dp4, in D) labial view, E) occlusal view, and F) lingual view; (G-I) CdP97 left M2, in G) labial view, H) occlusal view, and I) lingual view; (J-L) CdP99 left M2 in J) labial view, K) occlusal view, and L) lingual view; (M-O) CdP 101 right M3, in M) labial view, N) occlusal view, and O) lingual view; (P-R) CdP103 left M3, in P) labial view, Q) occlusal view, and R) lingual view. The scale bar equals 3 cm.

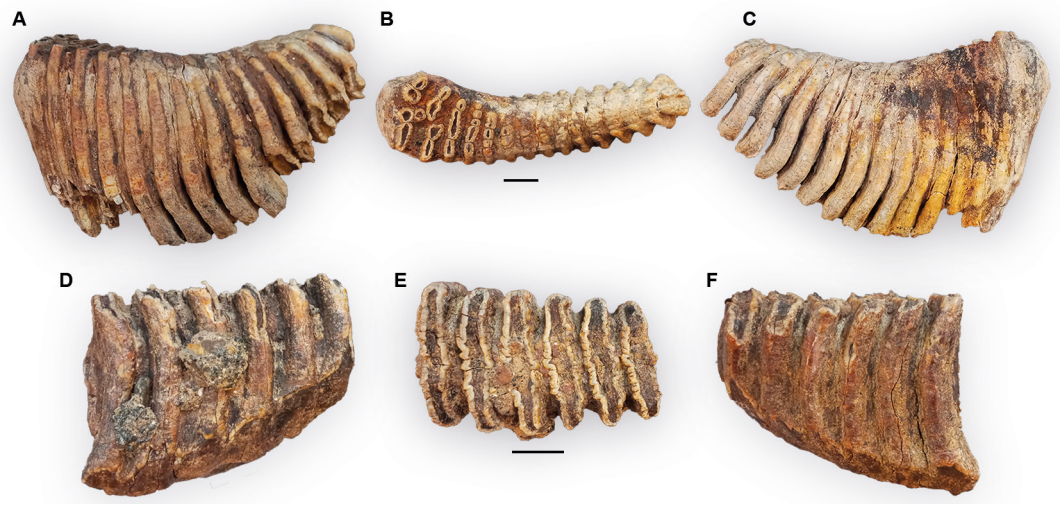

Fig. 2 - *Palaeoloxodon antiquus* lower teeth from Casal de'Pazzi. (A-C) CdP98 right m3, in A) labial view, B) occlusal view, and C) lingual view; (D-F) CdP100 right m3, in D) labial view, E) occlusal view, and F) lingual view. The scale bar equals 3 cm.

and tibia, and a pelvis fragment). The examined sample, comprised of the best-preserved specimens, consists of: CdP102, right tusk; CdP95 and CdP96, right PD4; CdP97 and CdP99, left M2; CdP101, right M3; CdP103, left M3; CdP98, right m3; and CdP100, right m3.

Description: The right tusk is almost complete, though an estimate of the length of the proximal portion inside the alveolus is hardly possible. The tusk is about 3 m long and with a maximum circumference of 64,5 cm (Tab. 1), gently curved, as indicated by the very high ratio of the length of the chord to the length measured on the external curvature (0.98). It is slightly pointed towards the sagittal plane, and very weakly upwards. The circumference gradually decreases from the proximal to the distal extremity, resulting in a narrow and pointed tip. All these morphological traits are typically observed in tusks of adult *P. antiquus* individuals. Moreover, the tusk is quite slender, less massive than in the most robust large males.

In both Dp4 deciduous teeth, all plates are in use, although CdP96 (Fig. 1 D-F) shows an advanced stage of wear, which caused the loss of some distal plates. The observed wear in CdP95 (Fig. 1 A-C) is less in comparison, preserving a higher crown, with the loss of the proximal plates being due to tooth breakage. In CdP95, the morphology of the enamel loops is somehow contradictory. In the less worn plates, a ring-loop-ring wear-facet can be observed, while in the intermediate plates, the size of the central loop decreases, and the two labial and lingual dots become slightly enlarged. On the anterior occlusal surface, the fully fused loops have one anterior and posterior pronounced midline fold, lacking additional medial and lateral large folds to the median ones, and the loops do not have the loxodont shape, typical of some *P. antiquus* molars. The quite advanced wear stage of the CdP96 deciduous premolar somehow reduces the diagnostic significance of the enamel loop features, though in the deepest worn plates, loops have a "cigar shape", which is not uncommon in *P. antiquus* molars (Herridge and Lister, 2012). The posterior plate is lingually displaced, and a small labial spur is present. Both premolars have rather thick, weakly folded enamel. The dimensions (Tab. 1) roughly conform to those of *P. antiquus* last premolars and are similar to those of Dp4 described by Maccagno (1962) (juvenile cranium n. 170), stored at the Palaeontological Museum (currently Museo Universitario di Scienze della Terra MUST, Sapienza Università di Roma).

CdP97 M2 (Fig. 1 G-I) is identified as a second upper molar, being characterized by its large size and by the presence of proximal surface contact with another tooth (Tab. 1). The molar counts 15 complete plates. Anteriorly, the tooth is worn to the dentine, though a small segment of the enamel loop of the most distal plate is still detectable. The presence of the proximal portion of the centrally placed first root allows us to identify this plate as the first of the tooth. As such, no plates are missing and 16 is the original plate number. The wear of the most posterior plates is just incipient, and dots are neither fused or incompletely fused. In a moderately worn plate, the two dots flanking the large median elliptical loop are derived from the wear of the dot-dash-dot *Palaeoloxodon* pattern. The intermediate plates are slightly curved towards the proximal side, while the distal ones are cigar-shaped and tightly packed together. The enamel is regularly and weakly folded, with no large folds present.

CdP99 M2 (Fig. 1 J-L) is deeply worn and proximally broken, and it may be a second last molar because the basal portion of the proximal surface is flattened by the pressure of the following tooth, likely a third molar. Its occlusal width is larger than that of the other CdP upper molars (Tab. 1), but the advanced wear limits the taxonomic value of its morphometric characters.

Tab. 1 - Tooth measurements of *Palaeoloxodon antiquus* teeth from Casal de'Pazzi.

Palaeoloxodon antiquus

Tusks - measurements in cm

Inventory Number	Maximum Length (external curvature)	Chord Length	Proximal Circumference	Circumference at 15 cm from the distal end	Chord Length/ Maximum length
CdP102 (almost complete)	315	308	64.5	25.5	0.98
CdP140 (incomplete)*	117	-	-	-	
CdP153 (incomplete)*	118	105	-	-	0.89
CdP154 (incomplete)*	169	-	-	-	-
CdP157 (incomplete)*	198	-	-	-	-
CdP167 (incomplete)*	290	284	-	-	
CdP175 (incomplete)*	132	-	-	-	-
CdP177 (largely incomplete)*	85	-	-	-	-
CdP181 (incomplete)*	130	-	-	-	-
CdP190 (incomplete)*	110	-	-	-	-

Premolars and molars - measurements in mm

Inventory Number	Tooth	Side	Plates			Length		Windth		Crown Heigth		Lamellar Frequency				Enamel tickness			Hypsodonty index (H/W)
			Formula	Total (PI)	in use (PlF)	Total (L)	Occlusal (LF)	Crown (W)	Occlusal (WF)	Crown (H)	Functional (HF)	Average (F)	Occlusal (Fo)	Labial (Fl)	Lingual (Fb)	Minimum (em)	Average (e)	Maximum (emax)	
CdP95/553628	Dp4	right	x 7+ ∞	>7	7.5	>107.80	>107.80	52.54	45.79	-	97.2	8	8	8	8	1.27	1.64	1.99	-
CdP96	Dp4	right	∞ +7 x	>7	7.5	>92.90	>92.90	50.57	47.47	-	>59	-	>7	-	-	1.67	1.99	2.26	-
CdP97/424898	M2	left	16 x	16	15	ca. 255	ca. 224	81.81	71.26	132	125	6	7	5	6	1.82	2.43	3.01	1.61
CdP99/424924	M2	left	x 6+ ∞	>6	7	-	>113.88		75.69	-	-	ca. 4.5	5	-	4	2.38	2.74	3.66	-
CdP101/426072	M3	right	∞ 11+ p	>11	10.5	>210	>168	78.69	73.62	113.67	101.93	5	5	5	5	2.50	2.97	3.37	1.44
CdP103/424896	M3	left	15 x	14.5	13	241.32	208.76	73.87	66.42	149.6	133.1	6	7	6	6	1.26	2.39	3.24	2.03
CdP98/550089	m3	right	x 14 x/p	14	7	ca. 260	86.98	68.9	59.93	ca. 175	-	5	6	5	5	2.00	2.60	3.25	ca. 1.5
CdP100	m3	right	∞ 6 ∞	>6	6	>142	>122	77.4	75.65	-	ca. 83	5	5	5	4	2.76	3.09	3.64	0.00

Abbreviations: *, specimen embedded in sediments; x, talon; p, platelet ; ∞, incomplete tooth due to wear or molar breack; +, incomplete plate; >, minimum measure of incomplete tooth; -, unable to measure.

The last upper molars (M3) CdP 101 (Fig. 1 M-O) and CdP103 (Fig. 1 P-R) have a narrow and high crown, progressively decreasing in height toward the rear. The observed loop features fall within the morphological variability of *Palaeoloxodon*. They preserve a rather similar stage of wear, which is a little less advanced in CdP103. The most anterior plates are the first one in CdP 101, and the second one in CdP. CdP101 is distally broken, preserving 11 complete plates and the proximal platelet. The roots are broken, and the poor preservation status prevents us from assessing the number of missing plates. CdP103 is nearly complete, the most anterior plate is worn till the base of the crown. The roots are broken near the base of the crown, and the first root is not clearly discernible. Thus, in this case, it is impossible to know if there are any missing plates. In the most posterior, less worn plates, loops show the typical dot-dash-dot pattern. In plates a little more worn, a long elliptical medial loop is flanked by lingual and labial dots, which partially blend with the medial loop with the increase of the wear. In the most worn plate, the loops are cigar shaped. The enamel is thicker, and the folds are rather large and more evident in CdP101 than in CdP103.

The m3 CdP98 (Fig. 2 A-C) is well preserved and partially erupted from the alveolus molar, which shows the anterior surface worn flat from the preceding m2 and plates are open at their bottom. The crown curvature, the narrowing of crown width, and the progressive decrease of its height towards the posterior sides of the tooth are diagnostic features of the lower molar of *P. antiquus*. The molar preserves 14 plates, seven in an early wear stage with a still unfused ring, and seven not in use, with a small platelet not extending to the crown base.

CdP100 is a largely incomplete m3 at a moderately advanced wear stage (Fig. 2 D-F). The proximal and distal plates are missing, and the roots are broken. The enamel is rather thick on the loops of the seven preserved plates, the enamel folds are large and clearly marked, and more prominent enamel folds are present on the loop median, which shows a moderate expansion on some plates.

Remarks: During the Middle Pleistocene, the Italian large mammal fossil record includes two continental elephant species: *Mammuthus trogontherii* (Pohlig, 1885), recovered from very few sites, and the more common *P. antiquus*, recorded especially during the second half of the Middle and early Late Pleistocene, when its remains were often the most abundant in local faunal assemblages (Palombo, 2023 this volume). The CdP dental remains show morphological features, such as the general shape of the tusk and chewing teeth, closer to those of *P. antiquus* than to those of *M. trogontherii*. Particularly in molars, the loops of the plates in an early wear stage show the characteristic dot-dash-dot pattern, with averagely worn plates frequently cigar-shaped. The crown is also rather high in poorly worn teeth. The lamellar frequency observed in the CdP dental remains is lower than the average frequency known for *M. trogontherii*, along with a thicker and less folded enamel, which shows an irregular folding pattern. Individual folds are rather loosely packed and of lesser amplitude, with large anterior and posterior folds flanked by distinct subsidiary folds sometimes present along the midline of the plates, though the "loxodont' form is hardly detectable. Accordingly, the morphologic and morphometric comparisons on the CdP elephant teeth, especially those of the tusk and upper molars, support the identification as *P. antiquus*. In particular, upper and lower last molars fall within the variation range of the rather small sample of Italian continental straight-tusked elephants analyzed by Palombo and Ferretti (2005). In the time frame when *P. antiquus* is recorded in the Italian fossil assemblages, a few differences in chewing tooth morphological features through time (e.g., enamel wear figures of the occlusal surface) have been noted by some authors (e.g., Palombo, 1986; Ferretti, 1998). However, such differences are possibly more related to intra-population individual variability than to any evolutionary trend.

Order Carnivora Bowdich, 1821
Family Canidae Fischer de Waldheim, 1817
Genus *Canis* Linnaeus, 1758
Canis cf. *lupus*, Fig. 3 A-I, Tab. 2

Material: CdP112, left hemimandible with p4-m2; CdP868, right lower carnassial (m1).

Description: The incomplete hemimandible (CdP112) is broken on the distal side between the alveolus of p2 and the canine. The p2, p3, and m3 are missing, and the premolar alveoli are damaged on their vestibular side (Fig. 3 A-C). The height of the horizontal ramus increases from p2 to m2, but it is not too deep (Tab. 2). The coronoid process is rather high, moderately medio distally large, and the coronoid crest is quite prominent; the condyle process is moderately robust and slightly inclined; the masseteric fossa extends till the distal edge al m3 but is not particularly deep; the angular process is moderately robust. All these features are commonly present in Middle Pleistocene *Canis* representatives.

The preserved teeth are in a moderately advanced stage of wearing, as the fairly large worn subplanar surfaces at the cusp top of the premolar and carnassial indicate. The mesio-lingual occlusal surface of m2 is damaged, but its advanced wear is still detectable. The p4 is slightly inclined, overlaps the carnassial vestibular side, and is rather robust but elliptical in shape. A small accessory cuspulid is present on the lingual side between the two main cusps, and some very small ones are observed on the distal cingulid (Fig. 3 D-F). A small cusp, more developed than in the other premolar, is also present on the distal cingulum of Lunel Viel specimens (Bonifay, 1971; Boudadi-Maligne, 2010, Fig. 131). The length and vestibol-linguar width of CdP p4 are similar to the values obtained for the small wolf, *Canis lupus lunellensis* Bonifay, 1971, from Lunel Viel (France) (Tab. 2). In the

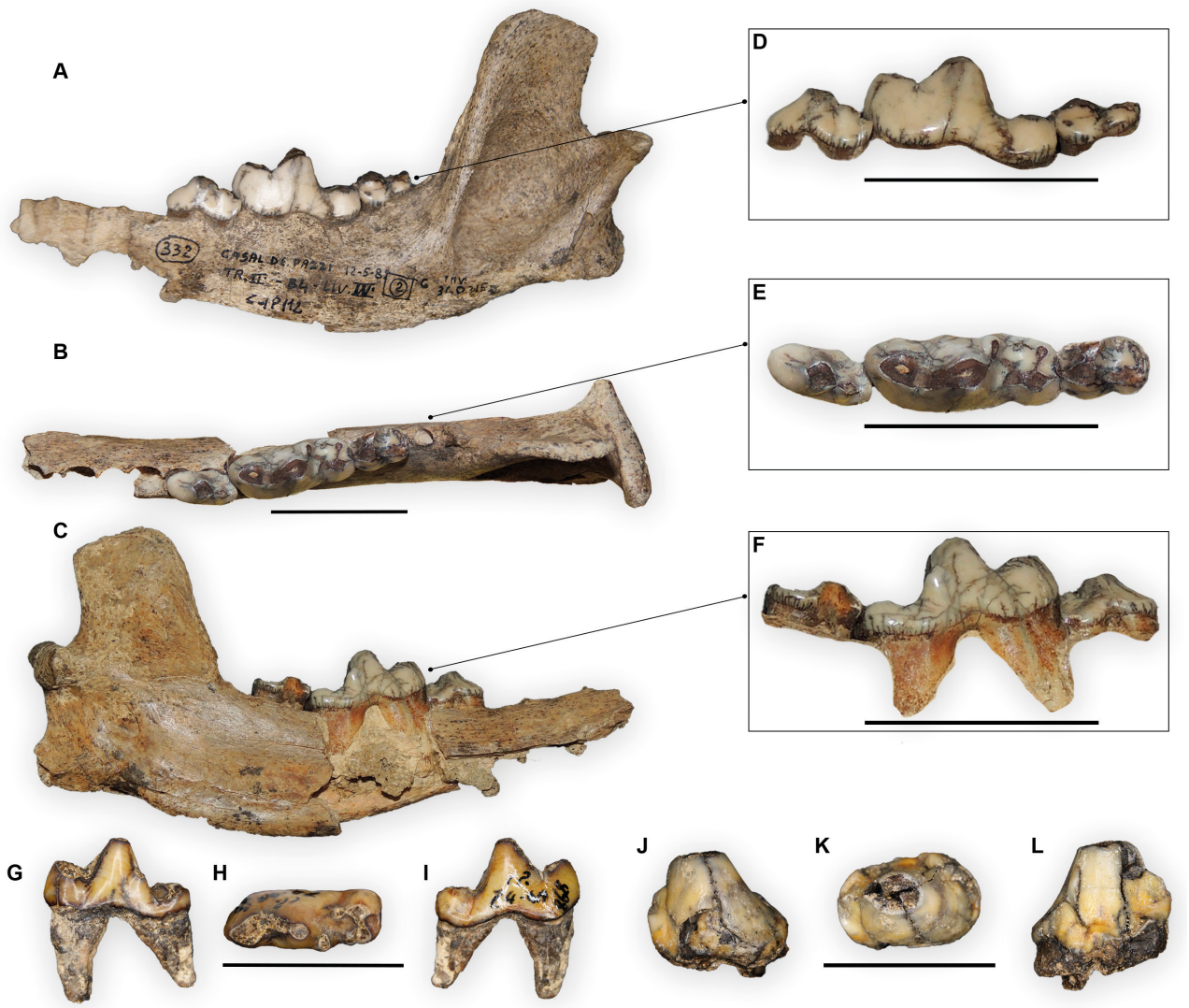

Fig. 3 - *Canis* cf. *lupus* from Casal de'Pazzi, (A-F) CdP112 left hemimandible with p4-m2 . (A-C) CdP112 hemimandible in A) labial view, B) occlusal view, and C) lingual view; (D-F) CdP112 lower tooth series in D) labial view, E) occlusal view, and F) lingual view; (G-I) CdP868 right lower carnassial in G) labial view, H) occlusal view, I) lingual view. *Crocuta* cf. *spelaea* from Casal de'Pazzi, (J-L) CdP1262785 P3 in J) labial view, K) occlusal view, and L) lingual view. The scale bar equals 3 cm.

lower carnassial trigonid, the paraconid and protoconid are large and stout, while the metaconid is reduced to a small cusp on the mandible lingual side. As a result, the first two cusps are aligned along a line concave toward the lingual side, while the position of the metaconid, not distally inclined, reduces the angular width among the three cusps. Thus, the angle is less obtuse than that observed in the Early Pleistocene *Canis* representatives, as well as in many *C. mosbachensis* Soergel, 1925 trigonids. In the CdP m1 (Fig. 3 G-I), the mesial margin paraconid is gently distally inclined, and in some specimens, its tip is higher than that of the p4 protoconid. The trigonid length of CdP112 m1 roughly equals the maximum value reported for the lower carnassial of the Lunel Viel sample, while that of CdP868 is higher than their average value (Tab. 2). The talonid is small; its mesio-distal length is about a quarter of the tooth's total length (26,8%), sub-quadrangular in shape, lower compared to the height of the trigonid cusps; the hypoconid is larger and higher than the entoconid; and the cingulum is weakly developed. The m2 is almost rectangular in shape, slightly broken on the lingual side possibly during the chewing process of hard food.

The main morphological features of teeth roughly conform to those of *C. lupus*, in particular those of *C. lupus lunellensis*, a subspecies with which the CdP teeth share a small dimension (Tab. 2).

The lower carnassial CdP868, which is just incipiently worn, basically has the same morphological features but is smaller, with less robust cusps despite its greater mesial vestibulo-lingual width. The length, indeed, is just inferior to the minimum value reported for the Lunel Viel sample, though even smaller m1 is reported in the *C. lupus* carnassials from a few Southern Italian sites (cf. Berté and Pandolfi, 2014, table 5, p. 374).

Tab. 2 - Measurements of *Canis* cf. *lupus* specimens from Casal de'Pazzi and comparison with *C. lupus* and *C. mosbachensis* from different Middle Pleistocene European sites.

Canis cf. *lupus* from Casal de' Pazzi

Hemimandible

Invent. n	Maximum length	Height of coronoid process	Articular condyle height	Height of the mandible below m1	Height of the mandible between m1/m2			
CdP112	43.04	59.1	31.53	24.47	25.40			

Lower teeth

Invent. n			Length	Vestibol-lingual width	Mesial vestibo-lingual width	Distal vestibo-lingual width	Occlusal length	Trigonid vestibo-lingual width	Talonid vestibo-lingual width	Trigonide Length	Talonid length
CdP112	p4		14.74	7.46	6.68	7.17	-	7.17	-	-	-
	m1		26.17	10.61	9.47	-	24.13	10.66	9.31	19.65	7.02
	m2		12.20	7.81	6.41	7.61	-	7.61	-	-	-
CdP868	m1		24.35	9.53	8.14	-	-	9.00	8.56	18.57	6.67

Canis lupus lunellensis from Lunel Viel (*)

Lower teeth

			Length	Vestibol-lingual width	Mesial vestibo-lingual width	Distal vestibo-lingual width	Occlusal length	Trigonid vestibo-lingual width	Talonid vestibo-lingual width	Trigonide Length	Talonid length
	p4	min	13.60	6.5	-	-	-	-	-	-	-
		M	14.50	7.1	-	-	-	-	-	-	-
		max	15.20	8.6	-	-	-	-	-	-	-
	m1	min	22.90	9.6	-	-	-	-	-	16.0	-
		M	25.00	10.2	-	-	-	-	-	17.9	-
		max	26.80	11.3	-	-	-	-	-	19.6	-
	m2	min	9.50	7.2	-	-	-	-	-	-	-
		M	10.20	7.8	-	-	-	-	-	-	-
		max	12.20	8.4	-	-	-	-	-	-	-

Canis mosbachensis from Untermassfeld (**)

			Length	Vestibol-lingual width	Mesial vestibo-lingual width	Distal vestibo-lingual width	Occlusal length	Trigonid vestibo-lingual width	Talonid vestibo-lingual width	Trigonide Length	Talonid length
	p4	min	12.50	5.70	-	-	-	-	-	-	-
		M	13.73	6.37	-	-	-	-	-	-	-
		max	14.90	7.20	-	-	-	-	-	-	-
	m1	min	23.40	10.00	-	-	-	-	-	-	-
		M	24.44	10.72	-	-	-	-	-	-	-
		max	25.90	11.8	-	-	-	-	-	-	-
	m2	min	8.80	7.00	-	-	-	-	-	-	-
		M	9.22	7.60	-	-	-	-	-	-	-
		max	10.20	8.10	-	-	-	-	-	-	-

Tab. 2 ...Continued

Canis mosbachensis from the l'Escale Cave - Ensamble 3 (*)

			Lower teeth								
			Length	Vestibol-lingual width	Mesial vestibo-lingual width	Distal vestibo-lingual width	Occlusal length	Trigonid vestibo-lingual width	Talonid vestibo-lingual width	Trigonide Length	Talonid length
	p4	min	11.70	5.30	-	-	-	-	-	-	-
		M	13.18	6.08	-	-	-	-	-	-	-
		max	14.20	6.60	-	-	-	-	-	-	-
	m1	min	20.70	8.20	-	-	-	-	-	14.30	-
		M	22.50	8.85	-	-	-	-	-	15.50	-
		max	23.00	9.40	-	-	-	-	-	16.00	-
	m2	min	9.30	6.70	-	-	-	-	-	-	-
		M	10.00	7.18	-	-	-	-	-	-	-
		max	10.80	7.60	-	-	-	-	-	-	-

Canis mosbachensis from the l'Escale Cave - Ensamble 5 (*)

			Lower teeth								
			Length	Vestibol-lingual width	Mesial vestibo-lingual width	Distal vestibo-lingual width	Occlusal length	Trigonid vestibo-lingual width	Talonid vestibo-lingual width	Trigonide Length	Talonid length
	p4	min	12.00	5.30	-	-	-	-	-	-	-
		M	13.12	6.31	-	-	-	-	-	-	-
		max	15.00	7.60	-	-	-	-	-	-	-
	m1	min	20.50	7.80	-	-	-	-	-	13.20	-
		M	22.26	8.79	-	-	-	-	-	15.76	-
		max	25.30	9.80	-	-	-	-	-	17.60	-
	m2	min	8.30	8.30	-	-	-	-	-	-	-
		M	9.87	7.04	-	-	-	-	-	-	-
		max	10.20	8.20	-	-	-	-	-	-	-

Remarks: Canis mosbachensis and *C. lupus,* coexisted for some time during the Middle Pleistocene (Palombo, 2023, and references therein). Whatever the phyletic relationships of *C. mosbachensis* with other Early Pleistocene canids should be, most authors regarded the two species as part of a single evolutionary lineage (Zrzavý et al., 2018 and references therein), but their morphological differences, especially the dental ones, have long been debated and remain ambiguously defined (Ghezzo et al., 2014). Although the size of *C. mobachensis* is generally smaller than that of wolves, especially the Late Pleistocene ones, Mosbach's canid and the small wolf could slightly overlap in some tooth dimensions. However, the dimensions of the CdP m1 fall in the range of the *C. lupus lunellensis* rich sample from the rather older French site of Lunel Viel (MIS 11), and those of CdP112 are larger than most *C. mosbachensis* m1 (cf. Brugal and Boudadi Maligne, 2011, p. 178, figure 7), but those of CdP868 also fall in the range of specimens from the German site of Untermassfeld (Sotnikova, 2010).

Considering these results and the available data which indicate that the *C. mosbachensis-C. lupus* transition likely occurred from MIS 12 to MIS 11 (Mecozzi et al., 2021; Palombo, 2023, and references therein) and that small-sized wolf populations occurred in southern Italy, we ascribe the CdP rather small remains to *Canis* cf. *lupus.*

Family Hyaenidae Gray, 1821
Genus *Crocuta* Kaup, 1828
Crocuta cf. *spelaea*, Fig. 3 J-L

Material: CdP1262785, P3; CdP348 (340310), MTIII.

Description: The P3 is robust and pyramidal. It shows a largely developed protocone, which is surrounded by a well-developed cingulum on the lingual margin and

lacks accessory cusps. The length and width values of P3 from CdP exceed the measurements of extant *C. crocuta* (Erxleben, 1777) (Fig. 4). The studied tooth is longer than *C. c. "praespelea"* (Schütt, 1971) and *C. intermedia* (De Serres et al., 1828) and proportionally narrow, but similar to *C. spelaea* (Ewer and Singer, 1956) (Fig. 4). The MTIII is damaged on its proximal-posterior side. The bone is relatively long, with the greatest length equalling 84.3 mm.

Remarks: According to a recent revision of the genus *Crocuta* carried out by Lewis and Werdelin (2022), the occurrence of the species *C. crocuta* can be traced back from the Late Pleistocene until recent days, and it is limited to the African continent. The Middle to Late Pleistocene European fossil *Crocuta* can instead be referred to two species: *C. intermedia* and *C. spelaea* (see Palombo, 2023 this volume). The length of MTIII falls within the values of *C. crocuta* and *C. spelaea* given by Sauqué et al. (2017), and the breadth of the shaft (10.93 mm) is close to the minimal values of both species. Considering the results of the morphometric comparison, we cautiously refer the CdP hyaena to *C. spelaea*.

Order Perissodactyla Owen, 1848
Family Equidae Gray, 1821
Tribe Equini Quinn, 1955
Genus *Equus* Linnaeus, 1758
Equus sp. Fig. 5 A-C, Tab. 3

Material: CdP113, upper right M1-2 or P3-4.

Description: The tooth (Fig. 5 A-C) shows marked signatures of protracted rolling and abrasion processes during fluvial transport that altered its dimensions and proportions, and erased some morphological details, such as the presence of sulci on styles. Moreover, the diagenetic process altered both dentine and enamel. As a result, no morphological details of the enamel figures on the occlusal surface are confidently detectable, and even the basic measurements given in table 3 are highly approximate.

The rather square shape of the tooth may suggest it could be a M1-2, though its apparently large paracone would indicate it could be a P3-4. The protocone outline is not clearly discernible, though the protocone seems to be rather elliptical in shape, moderately lengthened, symmetrical, and, perhaps, without lingual indentation. The shape and development of the caballine pli and the hypocone are not detectable. The outlines of the fossettes are vaguely defined, though the mesial one seems to be

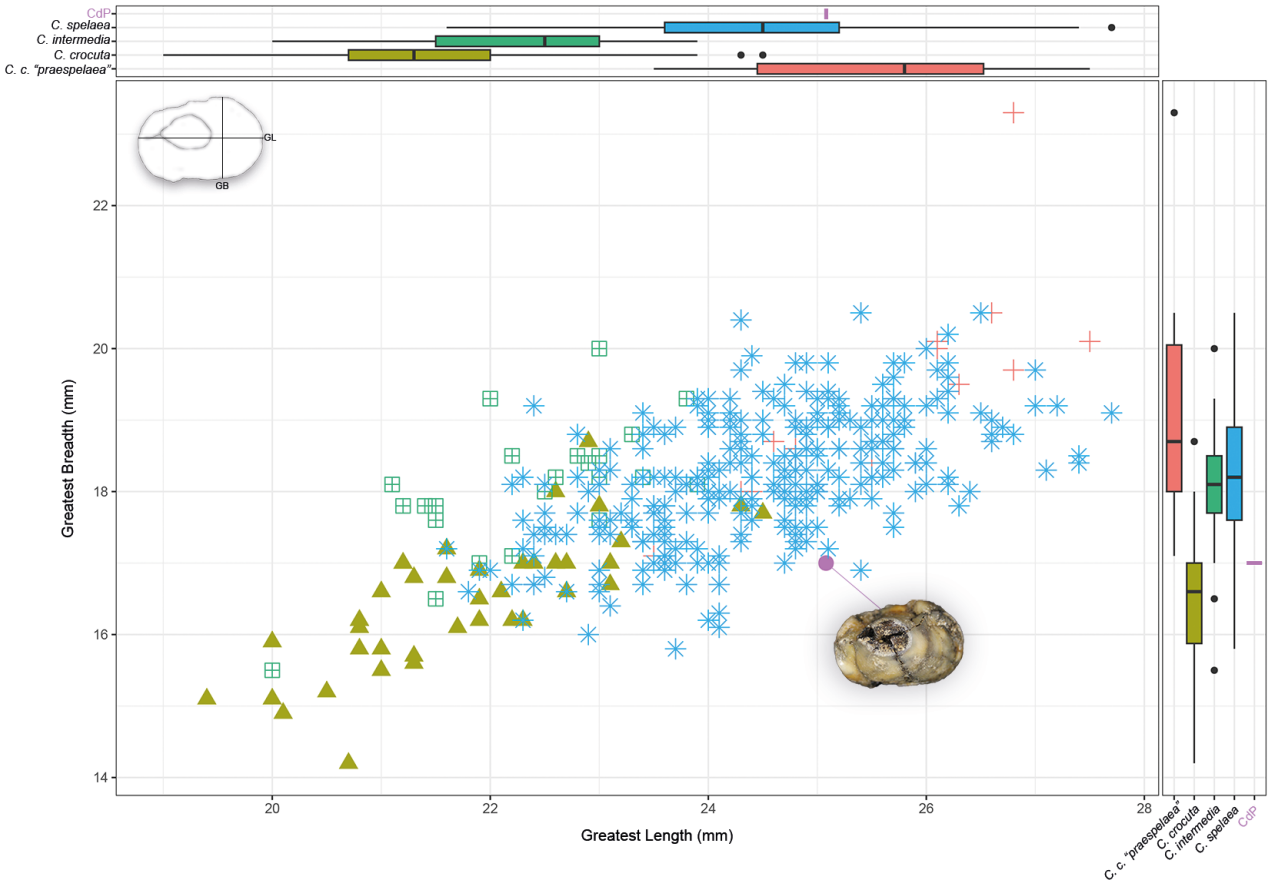

Fig. 4 - Bivariate diagram of greatest length (L) and greatest breadth (W), in mm, of P3 from CdP compared with *C. intermedia*, *C. c. "praespelaea"*, *C. spelaea* and *C. crocuta* (data from Lewis and Werdelin, 2022).

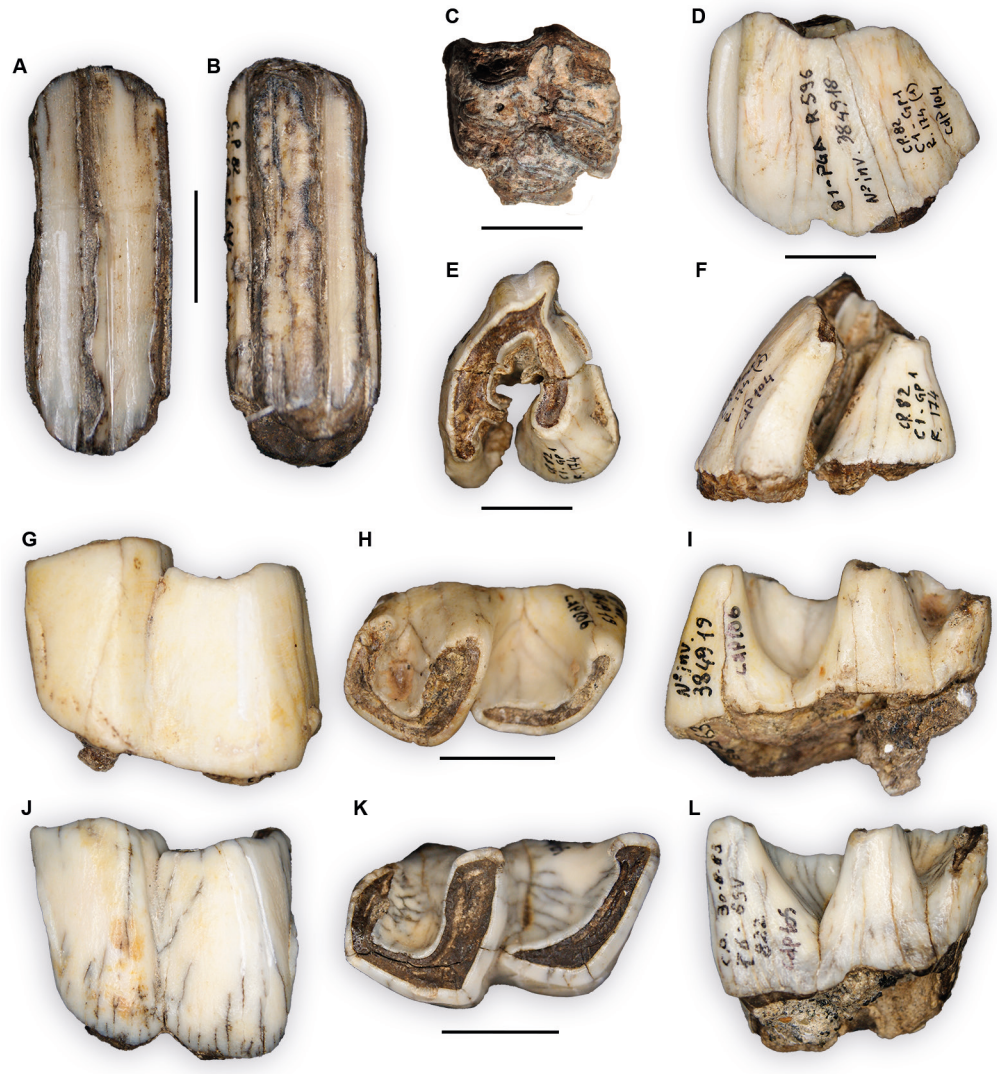

Fig. 5 - *Equus* sp. from Casal de'Pazzi, (A-C) CdP113 upper right M1-2 or P3-4, in A) labial view, B) occlusal view, and C) lingual view. *Stephanorhinus kirchbergensis* from Casal de'Pazzi, (D-F) CdP104 right M3, in D) labial view, E) occlusal view, and F) lingual view; (G-I) CdP105 left m1, in G) labial view, H) occlusal view, and I) lingual view; (J-L) CdP106 left m2, in J) labial view, K) occlusal view, and L) lingual view. The scale bar equals 2 cm.

Tab. 3 - Tooth measurements of *Equus* sp. from Casal de'Pazzi.

Equus sp.

Inventory Number	Tooth position	Side	Measurement (mm)				
			Occlusal length	Occusal breadth	Height	Protocone occlusal length	Protocone index
CdP113 (384908)	M1-2 (? P3-4)	Left	>26.51	ca. 26.15	73.11	ca. 12	ca.45.27

quite developed, maybe with a few plis.

Remarks: During the late Middle Pleistocene, three equids of different sizes were present in Italy, i.e., the small and slender *Equus hydruntinus* Regalia, 1905, whose phyletic relationships are a matter of debate (e.g., Boulbes and Aspersen, 2019; Cirilli et al., 2022 and references therein), and two caballine horses, the large, rather primitive *Equus mosbachensis* Von Reichenau, 1915 and the quite smaller and more advanced *Equus ferus* Linnaeus, 1758 (Palombo, 2023, and references therein).

In the published papers that provided the list of the species present in the CdP whole faunal sample, *E. hydruntinus* has never been mentioned, and the horse remains were commonly ascribed to *E. ferus*, suggesting they belong to a caballine horse. The measured length of the CdP tooth (Tab. 3), which is slightly inferior to the original one, is comparable with the minimum values reported for the majority of *E. mosbachensis* M1-2 specimens and smaller than those of the Mosbach's horse P3-4, except for *E. m. micoquii* Langlois, 2005 (Alberdi pers. comm.). The size of a horse's isolated tooth has, however, a modest diagnostic significance, especially if the tooth position is not firmly identified because, for instance, in *E. mosbachensis*, premolars are generally larger than molars, while the opposite occurs in *E. ferus* (Alberdi pers. comm.). The value of the protocone index is regarded as more compelling, being on average higher in *E. ferus* than in *E. mosbachensis*, though the variation ranges of the two species slightly overlap.

The protocone index inferred for the CdP tooth (45.26) falls in the range of both *E. mosbachensis* and *E. ferus*, but its actual value is hardly knowable because the tooth occlusal length is underestimated and the protocone length is just an estimate due to the protocone proximal and distal edges not being clearly demarcated and the occlusal surface being concave. Based on estimated hypothetical lengths, the value may range between >44.5 and <46.3.

Considering that the bad preservation status of the tooth increases the objective difficulties of identifying horse isolated chewing teeth due to their morphometric variation related to the wear degree and the inter- and intra-population differences, we leave open the identification of the CdP horse tooth.

Family Rhinocerotidae Gray, 1821

Genus *Stephanorhinus* Kretzoi, 1942

Stephanorhinus kirchbergensis (Jäger, 1839), Fig. 5 D-L, Tab. 4

Material: The material includes only isolated teeth: CdP104, right M3; CdP105, left m1; and CdP106, left m2.

Description: In the labial view (Fig. 5D), the M3 shows a long parastyle and a wide paracone fold. In the occlusal view (Fig. 5E), the ectometaloph profile on M3 is convex, with a faint paracone fold. The crochet is double, and the crista is well-developed. In the same view, the protocone is constricted and the mesial cingulum is present. The enamel is smooth, and the protocone, in lingual view (Fig. 5F), is large at its base. In the labial view, the enamel of the lower molars is smooth, and mesial and distal cingula are present (Fig. 5 G,J). In occlusal view, the lower molars show a wide labial groove and a curved talonid (Fig. 5 H, K). In the lingual view (Fig. 5 I,L), the lingual valleys are broad V-shaped on m1, while being U-shaped (posterior) and broad V-shaped (anterior) on m2.

Remarks: Usually, isolated teeth of Rhinocerotidae do not display useful characters for taxonomic identification. However, some species can be better distinguished from others because they are characterized by a combination of some peculiar features, observable on slightly or moderately worn teeth. *Stephanorhinus kirchbergensis*, here identified for the first time at CdP, can be diagnosed based on such a combination of characters: smooth enamel, faint paracone fold, broad lingual valleys, and wide labial groove. The smooth enamel of the M3 and the convex ectometaloph profile suggest an attribution to *S. kirchbergensis* rather than other Middle Pleistocene *Stephanorhinus* species, i.e., *S. hundsheimensis* (Toula, 1902) and *S. hemitoechus* (Falconer, 1859) (see Palombo, 2023 this volume), characterized by rough enamel and prominent paracone fold on the upper teeth and rough enamel, narrow lingual valleys, and narrow labial groove on the lower teeth (cfr. Guérin, 1980; Fortelius et al., 1993; Lacombat, 2005; Pandolfi, 2013; Pandolfi and Marra, 2015; Pandolfi et al., 2021; Pandolfi, 2023).

Tab. 4 - Tooth measurements of *Stephanorhinus kirchbergensis* from Casal de'Pazzi.

Stephanorhinus kirchbergensis

Inventory Number	Tooth position	Side	Measurement (mm)							
			Maximal length	Maximal width	Labial length	Lingual length	Mesial transverse diameter	Distal transverse diameter	Crown height	Height of anterior/ posterior valleys
CdP104 (384918)	M3	Right				44.67	52.55	60.33	47.62	
CdP105	m1	Left	45.54	28.98	40.26	41.75	26.00	27.50		15.94/13.29
CdP106	m2	Left	51.48	27.72	47.53	50.52	23.58	27.58		10.25/6.33

Order Cetartiodactyla
Family Hippopotamidae Gray, 1821
Genus *Hippopotamus* Linnaeus, 1758
Hippopotamus cf. *amphibius* Linnaeus, 1758, Fig. 6 A-M

Material: CdP107, left fragmented C; CdP867 B9.BG, left dp3; CdP108, left fragmented c; CdP110, left m3; CdP109, fragmented right m3.

Description: The upper canine (Fig. 6 A-C) has finely crenulated enamel and some longitudinal striae. In occlusal view, the upper canine shows a well-developed longitudinal groove. The crown is beveled due to its occlusion with the lower canine. The cross-section of the upper canine is bilobate. The lower canine (Fig. 6D) preserves the medial part, while the lateral one is missing. The medial part is characterized by finely crenulated enamel, longitudinal ridges, and a longitudinal groove. The dp3 (Fig. 6 E-G) is almost unworn and shows rough enamel. In occlusal view, three main cusps are visible: the protoconid, hypoconid, and entoconid. The protoconid is the bigger cusp, while in the distal part, the entoconid is slightly bigger than the hypoconid. The protoconid and the hypoconid are connected through the postprotocristid, and the hypoconid is slightly worn. The crenulated cingulid is particularly well-developed in distal view, while it is vaguely visible in labial and lingual view. In lingual view, a small metaconid is present on the lingual side of the tooth. The m3 CdP110 (Fig. 6 K-M), in occlusal view, shows five well-developed cuspids, and the hypoconid has a prehypocristid in connection with the metaconid and the protoconid. The m3 CdP110 is fairly worn, all the cuspids are characterized by a trefoil-wear pattern, while the hypoconulid shows a peculiar wear surface, more four-leaf clover or cruciform. The cingulid is well developed mesially, and a post-entostylid and a post-hypostylid are present distally. In the labial view, the cingulid is relatively developed, while it is completely absent in the lingual view similarly to CdP109 (Fig. 6 H-J). The latter specimen lacks the hypoconulid and shows a trefoil-wear pattern anterior cuspids, while the entoconid and the hypoconid are more comma-shaped.

Remarks: The hippo material mostly consists of incomplete specimens. The outlets of the transverse

Fig. 6 - *Hippopotamus* cf. *amphibius* from Casal de'Pazzi, (A-C) CdP107 left fragmented C in A) labial view, B) ventral view, and C) lingual view; (D) CdP108, left fragmented c in medial view; (E-G) CdP867 B9.BG, left dp3 in E) labial view, F) occlusal view, and G) lingual view; (H-J) CdP109, fragmented right m3 in H) labial view, I) occlusal view, and J) lingual view; (K-M) CdP110, left m3 in in K) labial view, L) occlusal view, and M) lingual view. *Sus scrofa* from Casal de'Pazzi, (N-P) CdP127 fragmented left c in N) lateral view, O) dorsal view, and P) medial view. The scale bar equals 2 cm.

valley on m3s are both V-shaped as in fossil and extant *H. amphibius* Linnaeus, 1758, while in other hippopotamids V-shaped and U-shaped combinations are both documented (Mazza, 1995; Martino et al., 2022). The hypoconulid of CdP110 shows a wear surface similar to that observed in the specimen C601 from La Maglianella and ascribed by Mazza (1991, 1995) to *H. tiberinus* Mazza, 1991. Mazza (1991) erected the species on material from La Maglianella (Rome), dated around 0.6 Ma, but its validity was later argued by Petronio (1995). Following Martino et al. (2022) the validity of *H. tiberinus* should be more thoroughly tested. The last occurrence of the latter species is still matter of discussion, since the remains dated around 0.5 Ma are particularly scarce and poorly preserved (Martino and Pandolfi, 2022). The dimensions of CdP110 fall within the variability of Middle to Late Pleistocene *H. amphibius*, being the Villafranchian *H. antiquus* Desmarest, 1822 characterized by larger dimensions (see Palombo, 2023 this volume). The posterior breadth, as well as the anterior one, is more similar to those of *H. amphibius* rather than *H. antiquus* (Fig. 7; Tab. S1, supplementary material). To sum up, the morphological

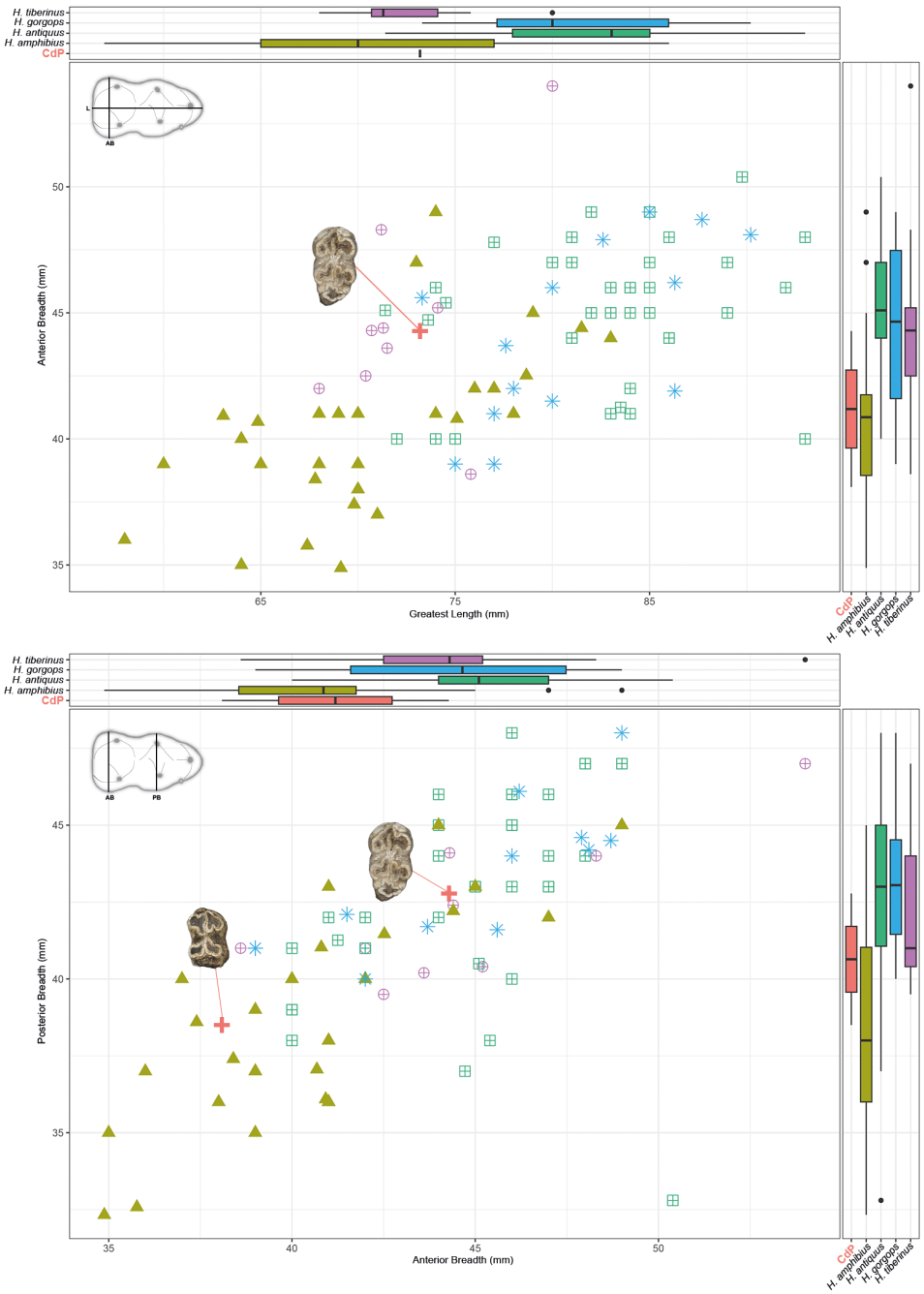

Fig. 7 - Bivariate diagram of m3s from CdP compared with *H. tiberinus*, *H. gorgops*, *H. antiquus*, and *H. amphibius*. A) Greatest Length vs. Anterior Breadth. B) Anterior Breadth vs. Posterior Breadth. (Data reported in Table S1, supplementary material, measurements in mm).

and morphometric features of the specimens collected from CdP are closer to *H. amphibius* rather than *H. antiquus*, however, a firm-specific attribution is avoided. Accordingly, the hippopotamid specimens from CdP are provisionally referred to *Hippopotamus* cf. *amphibius*.

Family Suidae Linnaeus, 1758
Genus *Sus* Linnaeus, 1758
Sus scrofa Linnaeus, 1758, Fig. 6 N-P

Material: CdP127, fragmented left c.

Description: A suid is represented by an apical fragment of a lower left canine (Fig. 6 N-P). The tooth has a strophic section. No other characters can be observed.

Remarks: The tooth clearly belongs to a species of suid, and it is referred to as *Sus scrofa* because it is the only species present in Europe during the Middle and Late Pleistocene (Martínez-Navarro et al., 2015; Palombo, 2023 this volume).

Family Cervidae Goldfuss, 1820
Genus *Cervus* Linnaeus, 1758

Cervus elaphus Linnaeus, 1758, Fig. 8 A-E
Material: CdP121, left fragmented basal antler; CdP123, right fragmented antler; CdP125, right m1 or m2; CdP122, left fragmented distal scapula.

Description: The antler remains show evident longitudinal grooves (Fig. 8 A-E). The specimen CdP123 is morphologically and morphometrically similar to CdP121, but it lacks the pedicle and most of the beam (Fig. 8 A-B). The basal antler portion of CdP121 (Fig. 8 C-E) displays a rounded burr, a brow tine, and a bez tine, but it lacks the trez tine. The brow tine is in contact with the burr. The fragment of the preserved pedicle is relatively long, and its posterior side forms an obtuse angle with the beam. In occlusal view, the lower molar displays a protoconid and hypoconid poorly separated antero-posteriorly, a straight posterior wing of the hypoconid, and strong lingual columns. The scapula preserves the distal articular surface and the glenoid tubercle. The glenoid cavity is smoothly rounded in distal view, and it is concave in the middle. The glenoid tubercle is well-developed and squared in lateral view, and the neck is short.

Fig. 8 - *Cervus elaphus* from Casal de'Pazzi: (A-B) CdP121, left fragmented basal antler in A) medial view and B) anterior view; (C-E) CdP123, right fragmented antler in C) medial view, D) lateral view, and E) anterior view. *Dama dama* from Casal de'Pazzi: (F-G) CdP126, right fragment of antler in F) medial view and G) lateral view. *Bos primigenius* from Casal de'Pazzi: (H) CdP85, right fragmented maxilla with P3-DP4-M1-M3 in occlusal view; (I) CdP86, right fragmented hemimandible with p1-p2-dp4-m1 in occlusal view; (J-L) CdP83, left m3 in J) labial view, K) occlusal view, and L) lingual view; (M-N) CdP91, right metacarpus in M) anterior view and N) posterior view; (O-Q) CdP89, right astragalus in O) anterior view and Q) posterior view. The scale bar equals 4 cm for A-G and 2 cm for H-Q.

Remarks: The antler morphology clearly supports the presence of the red deer at CdP. However, the material does not allow an attribution to one of the Middle Pleistocene subspecies (Palombo, 2023) recognized in Italy during the past century by several authors (Di Stefano and Petronio, 2021 and references therein). Only the presence of the bez tine allows to exclude *C. elaphus aretinus* Azzaroli, 1961. The isolated lower molar and the scapula can be generically assigned to the red deer due to their morphology (e.g., strong lingual columns, smoothly rounded glenoid cavity) and size (larger than *Dama* sp. and *Capreolus* Gray, 1821) (Lister, 1996b). No other considerations are currently possible. The presence of different subspecies has been primarily based on antler morphology and, in particular, on the morphology of the distal portion of the beam. Although some postcranial remains seem to be somehow useful to discriminate among some subspecies, e.g., *C. e. acoronatus* Beninde, 1937-*C. elaphus* ssp. (Di Stefano and Petronio, 1992, 1993; Di Stefano et al., 1992, 2015), no data are available at present for the scapula of these taxa. The remains from CdP are therefore too scarce and fragmented for any kind of consideration.

Genus *Dama* Frisch, 1775
Dama dama (Linnaeus, 1758), Fig. 8 F-G

Material: CdP126, a right fragment of an antler; CdP384861, a left fragment of an antler; CdP124, right m1 or m2; CdP117, left distal portion of scapula; CdP118, left fragmented radius; CdP119, right fragmented metacarpus; CdP120, first phalanx.

Description: The basal portion of the antler (Fig. 8 F-G) displays a brow tine that makes an oblique angle with the beam; the bez tine is absent, the beam makes an acute angle with the burr, and pearling and grooves are absent on the beam. In the occlusal view, the lower molar displays protoconid and hypoconid antero-posteriorly separated, no additional folds, slightly sinuous posterior wing of the hypoconid, and faint lingual columns. In the lingual view, the ectostyle is present, the anterior cingulum is well-developed, and the posterior cingulum is absent. In the distal view, the glenoid cavity of the scapula has a laterally flattening outline, and, on the lateral side, a widespread hollow is present in the posterior-distal portion of the bone. When observed in a distal view, the distal epiphysis of the radius shows a convex anterior border of the medial articular facet, while in the anterior view shows a thin ridge of the anterior-lateral side. The metacarpus only preserves the diaphysis and the distal epiphysis. The bone is rather long and slender, and the distal spit is not visible. The first phalanx is relatively long and narrow, and in the proximal view the articular facets for the articulation with the metapodial are poorly separated posteriorly.

Remarks: The morphology of the antlers discovered at CdP enable us to exclude the presence of *Dama clactoniana* (Falconer, 1868) and instead confirm the occurrence of *Dama dama* ssp. (see Palombo, 2023 this volume). The fragmented antler housed at MCP clearly belongs to the genus *Dama* and differs from those of *C. elaphus* (see previous remarks) and other large-sized cervids e.g., *Megaloceros giganteus* (Blumenbach, 1799), characterized by a flattened brow tine (Di Stefano, 1995; Lister, 1996b). The studied postcranial remains (Tab. S2, supplementary material) are larger than *C. capreolus* and generally smaller than *C. elaphus*. Their dimensions fit well with those of the fallow deer. The available measurements of the metacarpal (TDS=19.04 mm; DTD=32.11 mm) fall within the variability of the three late Middle and Late Pleistocene fallow deers, *D. dama tiberina* Di Stefano and Petronio, 1997 (n.=2; TDS=19-20.10 mm; DTD=32.10-32.30 mm), *D. dama dama* (Linnaeus, 1758) (n.=39; TDS=14-22.30 mm; DTD=25-33.40 mm), and *D. clactoniana* (n.=30; TDS=16.60-24.50 mm; DTD=31-37 mm), as well as the measurements of the radius (TDS=23.21 mm, DTD=35.41 mm; *D. dama tiberina*, n.=3, TDS=23.20-26.50 mm, DTD=35-37.50 mm; *D. dama dama*, n.=31, TDS=16-27.20 mm, DTD=30-42 mm; *D. clactoniana*, n.=15, TDS=17.60-30.80 mm, DTD=34.60-44 mm) (data from Leonardi and Petronio, 1976; Di Stefano, 1994). Following the diagnosis reported by Di Stefano and Petronio (1997), the morphology of the m1 would suggest a resemblance with *D. dama tiberina* due to the absence of a posterior cingulum, the presence of the ectostyle, and the presence of the anterior cingulum. However, we avoid a certain subspecific attribution based only on an isolated tooth.

Family Bovidae Gray, 1821
Genus *Bos* Linnaeus, 1758
Bos primigenius Bojanus, 1825, Fig. 8 H-N

Material: CdP170, fragmented occiput; CdP85, right fragmented maxilla with P3-DP4-M1-M3; CdP86, right fragmented hemimandible with p1-p2-dp4-m1; CdP81, right i; CdP82, right i; CdP83, left m3; CdP84, right M3; CdP87, atlas; CdP155, cervical vertebra; CdP90, lumbar vertebra; CdP94, left fragmented distal radius; CdP91, right metacarpus; CdP93, right fragmented femur distal epiphysis; CdP92, right fragmented distal tibia; CdP89, right astragalus; CdP88, third phalanx.

Description: The upper and lower teeth have a columnar shape without any kind of swelling at the base of the enamel (Fig. 8 H-L). The entostyle on the upper molars is well-developed, but on m3, the entostylid is not particularly developed. The upper molars have a quadrangular shape in the occlusal view, and the protocone and hypocone are wide (Fig. 8H). Metacone and paracone folds are developed and relatively wide. Similarly, the metaconid and entoconid on the lower molars are wide and rounded, and the hypoconulid is well-developed (Fig. 8 I-L). The lingual side of the lower incisors is flat and featureless. In the distal view, the distal epiphysis of the radius has the

anterior and posterior borders longer than the lateral and medial ones, and the distal anterior face has two barely visible parallel ridges. The articulations for the cuboid and the intermediate are similar in width, and that for the scaphoid is narrow and extends further posteriorly on the distal epiphysis. In the anterior view, the indentation for the articulation with the os carpi radiale is faint. The metacarpal bone has a long diaphysis and expanded epiphyses (Fig. 8 M-N). In the proximal view, there are two large articular facets posteriorly separated by a narrow groove, with an evident nutrient foramen in the middle. In the same view, the posteriormedial tubercle is moderately developed. In the anterior view, the vascular groove extends below the nutrient foramen near the distal end, and the transverse diameter of the distal articulation is wider than the suprarticular ones. The diaphysis is flat on its posterior side, and its transverse diameter is greater than its antero-posterior ones. The distal epiphysis of the femur is massive; the medial lip of the trochlea is not preserved, but it is clearly larger and extends more proximally than the lateral one. In the anterior view, the fossa patellaris is not evident. In the distal view, the distal articular surfaces on the tibia are parallel, with the medial articulation narrower and longer than the lateral ones, and the posterior border of the distal epiphysis slightly concave. The groove for the flexor digitalis is prominent, and the malleolar facet is narrow and confluent with the posterior facet. In the posterior view, the astragalus (Fig. 8O-Q) shows a curved lateral border of the posterior articular surface, and the posterior nutrient foramen opens directly outward. The distal border of the distal articulation is very distinct, and in the proximal trochlea the angle between the lateral and medial lips is V-shaped. In the lateral view, the facet for the calcaneus is long and narrow. The third phalanx has a curved planum cutaneum of the facies solaris.

Remarks: The bovid material from CdP clearly belongs to *B. primigenius* (see Palombo, 2023 this volume). Among the other features, the studied specimens can be distinguished from *Bison* Hamilton-Smith, 1827, which is characterized by a swelling base of the enamel on the teeth, poorly developed entostyle, and sharper metacone and paracone folds on the upper teeth. In addition, the morphology of the preserved postcranial remains fits well with the morphological features observed on auroch and listed by, among others, Brugal (1985), Sala (1986), and Gee (1993). The transverse and antero-posterior diameters of the distal epiphysis of the tibia (Tab. S2, supplementary material) are smaller than those of *B. primigenius* from Avetrana (n=11; DTD=80-85 mm, data from Pandolfi et al., 2013), and male and female individuals from Lunel Viel (respectively: DTD=78.1-90.2 mm; DAPD=57.9-75.2 mm and DTD=73.4-80 mm; DAPD=58.3-67.5 mm, data from Brugal, 1985). Such small dimensions are recorded at Grotta Romanelli and Barche (Tagliacozzo, 2003) but can be related to the presence of juveniles. The astragalus (Tab. S2, supplementary material) fits within the lowest values given for Pleistocene auroch populations (Lunel Viel: Hlat=81.7-100.8 mm; Hmed=74.2-93.8 mm; DTD=50.5-75.2 mm; APDM=45-57.2 mm) (Avetrana, n=24: Hlat=80-93 mm; Hmed=73-87 mm; DTD=51-63 mm; APDM=47.5-55 mm) (Aurelia, n=24: Hlat=78.7-99.2 mm; Hmed=73-91.8 mm; DTD=53.3-69.9 mm; APDM=38.1-52.5 mm). The distal transverse diameter of the metacarpus (Tab. S2, supplementary material) falls within the range of male individuals from Lunel Viel (DTD=85.4-99.2 mm) and is larger than that of females from the same locality (DTD=70.7-81.7 mm). The maximal length of m3 (Tab. S2, supplementary material) is close to the minimal values of *B. primigenius* from Paglicci (n=21; L=46-52.8 mm). At CdP, it is possible to attest the presence of at least a male individual of *B. primigenius*, represented by a large distal epiphysis of a metacarpal, and of several subadults or females, represented by small-sized postcranial elements and a fragmented mandible with dp4.

4. CONCLUSIONS

The mammal fauna either retrieved or still embedded in sediments of the CdP site is here described and compared for the first time after its excavation. The morphological and morphometric comparisons allow to document the presence of the following taxa: *Palaeoloxodon antiquus*, *Canis* cf. *lupus*, *Crocuta* cf. *spelaea*, *Equus* sp., *Stephanorhinus kirchbergensis*, *Hippopotamus* cf. *amphibius*, *Sus scrofa*, *Cervus elaphus*, *Dama dama,* and *Bos primigenius*.

Compared with previous published faunal lists, we discard the presence of ? *Canis* sp. aff. *C. arnensis* and *Crocuta crocuta* and instead report the occurrence of *Crocuta* cf. *spelaea*, and *Stephanorhinus kirchbergensis*. Unfortunately, the available material prevents us to unquestionably assign some taxa such as horse, red deer, and fallow deer, to a specific or subspecific level. We reject the presence in the CdP mammalian fauna of *Capreolus capreolus* and *Equus ferus*, which could be confidently documented by the material stored at the Soprintendenza Speciale Archeologia Belle Arti e Paesaggio di Roma. Similarly, we cannot confirm the occurrence of *D. dama tiberina* because the fallow deer sample documented in this study includes poorly diagnostic material.

A detailed study of the specimens so far unavailable will probably permit a compelling definition of the actual taxonomic composition of the mammalian assemblage from the site.

ACKNOWLEDGEMENTS - We are grateful to the Organizing Committee of the conference “40 years of Casal de’ Pazzi” and the Editor of the Journal of Mediterranean Earth Sciences for their interest in this contribution. We thank P. Gioia, G. Zanzi and L. Silvestri (Sovrintendenza di Roma Capitale) for access to the paleontological collection at MCP. R.M. benefited from the GeoBioTec NOVA grant UIDB/04035/2020 and PhD fellowship 2021.08458.BD by the Fundação para a Ciência e Tecnologia. We

thank M.T. Alberdi for her usefully advice on *Equus* molar, and T. Kotsakis and an anonymous reviewer for their constructive comments and suggestions. We also thank A. de Sousa Saleiro Barros for his advice on the text.

REFERENCES

Accordi B., 1955. *Hippopotamus pentlandi* von Meyer del Pleistocene della Sicilia. Palaeontographia Italica 50, 1-52.

Aguirre E., 1969. Revisión sistemática de los Elephantidae por su morfología y morfometría dentaria. Estudios Geológicos 25, 123-177 and 317-367.

Albayrak E., Lister A.M., 2012. Dental remains of fossil elephants from Turkey. Quaternary International 276, 198-211.

Antoine P.O., 2002. Phylogénie et évolution des Elasmotheriina (Mammalia, Rhinocerotidae). Mémoires du Muséum Nationale d'Histoire Naturelle 188, 1-369.

Anzidei A.P., Arnoldus Huizendveld A., Caloi L., Palombo M.R., Lemorini C., 1999. Two Middle Pleistocene sites near Rome (Italy): La Polledrara di Cecanibbio and Rebibbia-Casal De'Pazzi. In: The Role of Early Humans in The Accumulation of European Lower and Middle Palaeolithic Bone Assemblages. Monographien des Römisch-Germanischen Zentralmuseum 42, 173-195.

Anzidei A.P., Bietti A., Cassoli P., Ruffo M., Segre A.G., 1984. Risultati preliminari dello scavo in un deposito pleistocenico in località Rebibbia Casal de Pazzi (Roma). Atti della XXIV Riunione Scientifica: Il Paleolitico e il Mesolitico nel Lazio. Istituto Italiano di Preistoria e Protostoria, 131-139, Firenze.

Anzidei A.P., Gioia P., 1990. The lithic industry from Rebibbia-Casal de' Pazzi. In: Herring E., Whitehouse D.R., Wilkins J.B. (Eds.), Paper of the Fourth Conference of Italian Archaeology, New Development in Italian Archaeology, Part 1. Accordia Research Centre, London, 155-179.

Anzidei A.P., Gioia P., Mussi M., 2004. Uomini ed elefanti nel territorio romano: una lunga convivenza. La documentazione dai siti. In: Gioia P. (Ed.), Elefanti a Roma. Palombi editori, Roma, 49-57.

Berte D.F., Pandolfi L., 2014. *Canis lupus* (Mammalia, Canidae) from the Late Pleistocene deposit of Avetrana (Taranto, Southern Italy). Rivista Italiana di Paleontologia e Stratigrafia 120, 367-379.

Bowditch T.E., 1821. An analysis of the natural classifications of Mammalia for the use of students and travelers. J. Smith, Paris, pp.115.

Boisserie J.R., Lihoreau F., Orliac M., Fisher R.E., Weston E.M., Ducrocq S., 2010. Morphology and phylogenetic relationships of the earliest known hippopotamids (Cetartiodactyla, Hippopotamidae, Kenyapotaminae). Zoological Journal of the Linnean Society 158, 325-366.

Bojanus L.H., 1825. De uro nostrato ejusque sceleto commentatio Bovis primigenii sceleto aucta. Palaeontology Library of Muséum National d'Histoire Naturelle, Paris, pp. 53.

Bonifay M.F., 1971. Carnivores quaternaires du Sud-est de la France. Mémoires du Muséum Nationale d'Histoire, Série C 21, 43-377.

Boudadi-Maligne M., 2010. Les Canis pléistocènes du Sud de la France: approche biosystématique, évolutive et biochronologique. Ph.D Thesis, Université Bordeaux, Bordeaux, France 1, pp. 451.

Boulbes N., van Asperen E., 2019. Biostratigraphy and palaeoecology of European *Equus*. Frontiers in Ecology and Evolution 7, 301.

Brugal J.P., 1985. Le *Bos primigenius* BOJ. 1827 du Pléistocène Moyen des grottes de Lunel Viel (Herault). Bulletin Musée d'Anthropologie Préhistorique de Monaco 28, 7-62.

Brugal J.P., Boudadi-Maligne M., 2011. Quaternary small to large canids in Europe: taxonomic status and biochronological contribution. Quaternary International 243, 171-182.

Caloi L., Palombo M.R., Petronio C., 1980. Resti cranici di *Hippopotamus antiquus* (= *H. major*) e *Hippopotamus amphibius* conservati nel Museo di Paleontologia dell'Università di Roma. Geologica Romana 19, 91-119.

Caloi L., Palombo M.R., Zarlenga F., 1998. Late Middle Pleistocene mammal faunas of Latium (Central Italy): stratigraphy and environment. Quaternary International 47/48, 77-86.

Cirilli O., Machado H., Arroyo-Cabrales J., Barrón-Ortiz C.I., Davis E., Jass C.N., Jukar A.M., Landry Z., Marín-Leyva A.H., Pandolfi L., Pushkina D., Rook L., Saarinen J., Scott E., Semprebon G., Strani F., Villavicencio N.A., Kaya F., Bernor R.L., 2022. Evolution of the Family Equidae, Subfamily Equinae, in North, Central and South America, Eurasia and Africa during the Plio-Pleistocene. Biology 11, 1258.

Di Stefano G., 1994. Il daino pleistocenico dell'Eurasia. Ph.D Thesis, SAPIENZA Università di Roma, pp. 270.

Di Stefano G., 1995. Identification of fallow deer remains on the basis of its skeletal features: taxonomical considerations. Bollettino della Società Paleontologica Italiana 34, 323-331.

Di Stefano G., Leonardi G., Petronio C., 1992. New biometric data on *Cervus elaphus acoronatus* (Beninde, 1937). In: Spitz F., Janeau G., Gonzalez G. Aulagnier S. (Eds.), Ongulés/ Ungulates 91, 43-47, Paris-Toulouse.

Di Stefano G., Pandolfi L., Petronio C., Salari L., 2015. The morphometry and the occurrence of *Cervus elaphus* (Mammalia, Cervidae) from the Late Pleistocene of the Italian Peninsula. Rivista Italiana di Paleontologia e Stratigrafia 121, 103-120.

Di Stefano G., Petronio C., 1992. Nuove osservazioni su *Cervus elaphus acoronatus* Beninde del Pleistocene europeo. Bollettino della Società Paleontologica Italiana 31, 295-315.

Di Stefano G., Petronio C., 1993. A new *Cervus elaphus* subspecies of Middle Pleistocene age. Neues Jahrbuch für Geologie und Paläontologie, Abhandlungen 190, 1-18.

Di Stefano G., Petronio C., 1997. Origin and evolution of the European fallow deer (*Dama*, Pleistocene). Neues Jahrbuch für Geologie und Paläontologie, Abhandlungen 203, 57-75.

Di Stefano G., Petronio C., 2021. Importance of the morphological plasticity of *Cervus elaphus* in the biochronology of the Middle and Late Pleistocene of the Italian peninsula. Naturwissenschaten 108, 40.

Driesch A. von den, 1976. A Guide to the Measurement of Animal Bones from Archaeological Sites. Peabody Museum Bulletin 1, Harvard University, pp. 136.

Falconer H., Cautley P.T., 1845-49. Fauna antiqua sivalensis,

being the fossil zoology of the Sewalik Hills, in the north of India. 1845: Part I., 1846: Part II., 1847: Part III-VIII., 1849: Part IX., Smith Elder and Co., London.

Ferretti M.P., 1998. Gli elefanti del Plio-Pleistocene dell'Italia. Ph.D Thesis, Modena, Bologna, Firenze, and Roma Associated Universities, Italy, pp. 119.

Fischer von Waldheim G., 1817. Adversaria zoologica. Memoires de la Societe Imperiale des Naturalistes de Moscou 5, 368-428.

Fortelius M., Mazza P., Sala B., 1993. *Stephanorhinus* (Mammalia: Rhinocerotidae) of the Western European Pleistocene, with a revision of *S. etruscus*, Falconer, 1868. Palaeontographia Italica 80, 63-155.

Frisch J.L., 1775. Das Natur-System der vierfüßigen Thiere, in Tabellen, darinnen alle Ordnungen, Geschlechte und Arten, nicht nur mit bestimmenden Benennungen, sondern beygesetzten unterscheidenden Kennzeichen angezeigt werden, zum Nutzen der erwachsenen Schuljugend. Glogau (Günther Verlag), pp. 805.

Galobart À., Ros X., Maroto J., Vila B., 2003. Descripción del material de hipopótamo (*Hippopotamus antiquus* Desmarest, 1822) de los yacimientos del Pleistoceno inferior de Incarcal (Girona, NE de la Península Ibérica). Paleontologia i Evolució 34, 153-173.

Gee H.E., 1993. The distinction between postcranial bones of *Bos primigenius* Bojanus, 1827 and *Bison priscus* Bojanus, 1827 from the British Pleistocene and the taxonomic status of *Bos* and *Bison*. Journal of Quaternary Science 8, 79-92.

Ghezzo E., Bertè D.F., Sala B., 2014. The revaluation of Galerian Canidae, Felidae and Mustelidae of the Cerè Cave (Verona, northeastern Italy). Quaternary International 339-340, 76-89.

Gioia P., 2004. Il Museo di Casal de' Pazzi. In: Gioia P., (Ed.) Elefanti a Roma, Palombi editori, Roma, 61-63.

Gioia P., Persiani C., 2011. Museo di Casal de' Pazzi (deposito pleistocenico). Romàntìca, 4, 45-47, Milano.

Goldfuss G.A., 1820. Handbuch der Zoologie. In: Schubert GH (Ed), Handbuch der Naturgeschichte, zum Gebrauch bei Vorlesungen. Erste Abteilung, pp. 696, pls. 1-2; Zweite Abteilung, xxiv+ pp. 510.

Gray J.E., 1821. On the natural arrangement of vertebrose animals. London Medical Repository 15, 296-310.

Guérin C., 1980. Les Rhinocéros, Mammalia, Perissodactyla) du Miocène terminal au Pléistocène supérieur en Europe Occidentale. Comparaison avec les espèces actuelles. Documents des Laboratoires de Géologie, Lyon 79, 1-1185.

Harris J.M., 1991. Family Hippopotamidae. In: Harris, J.M. (Ed.), Koobi Fora Research Project, vol. 3: Stratigraphy, Artiodactyls and Paleoenvironments. Oxford, 31-85.

Herridge V.L., Lister A.M. 2012. Extreme insular dwarfism evolved in a mammoth. Proceedings of the Royal Society B 279, 3193-3200.

Hooijer D.A., 1950. The fossil Hippopotamidae of Asia, with notes on the Recent species. Zoologische Verhandelingen 8, 1-124.

Jäger G.F., 1839. Über die fossilen Säugethiere welche in Würtemberg in verschiedenen Formationen aufgefunden worden sind, nebst geognotischen Bemerkungen über diese Formationen. Carl Erhard, Stuttgart, pp. 214.

Kotsakis T., Barisone G., 2008. Cenni sui vertebrati fossili di Roma. Memorie Descrittive della Carta Geologica d'Italia 80, 115-143.

Kaup J.J., 1828. Über *Hyaena*, *Uromastix*, *Basiliscus*, *Corythaeolus*, *Acontias*. Isis 21, columns 1144-1150.

Kretzoi M., 1942. Bemerkungen zum System der nachmiozänen Nashorn-Gattungen. Földtani Közlöny 72, 4-12.

Illiger C.D., 1811. Prodromus Systematis Mammalium et Avium Additis Terminis Zoographicis Uttriusque Classis. Salfeld, Berlin, pp. 145-301.

Lacombat F., 2005. Les Rhinocéros fossiles des sites préhistoriques de l'Europe Méditerranéenne et du Massif Central – Paléontologie et implications biochronologiques. BAR International Series 1419, 1-175.

Leonardi G., Petronio C., 1976. The fallow deer of European Pleistocene. Geologica Romana 25, 1-67.

Lewis M.E., Werdelin L., 2022. A revision of the genus *Crocuta* (Mammalia, Hyaenidae). Palaeontographica Abteilung A 322, 1-115.

Linnaeus C., 1758. Systema Naturae per Regna Triae Naturae, secundum classes, ordines, genera, species, cum characteribus, differentiis, synonymis, locis. Edn 10. Laurentii Salvii, Holmiae, i-iv, pp. 824.

Lister A.M., 1996a. Evolution and taxonomy of Eurasian mammoths. In: Shoshani J., Tassy P. (Eds.), The Proboscidea: Evolution and Palaeoecology of Elephants and Their Relatives. Oxford University Press, Oxford, pp. 203-213.

Lister A.M., 1996b. The morphological distinction between bone and teeth of fallow deer (Dama dama) and red deer (*Cervus elaphus*). International Journal of Osteoarchaeology 6, 119-143.

Lister A.M., Van Essen H., 2003. *Mammuthus rumanus* (Stefanescu), the earliest mammoth in Europe. In: Petculescu A., Stiuca E. (Eds.), Advances in Vertebrate Paleontology "Hen to Panta". Institute of Speleology, Bucharest, pp. 46-52.

Maccagno A.M., 1962. Gli elefanti fossili di Riano (Roma). Geologica Romana 1, 33-132.

Maglio V.J., 1973. Origin and evolution of the Elephantidae. Transactions of the American Philosophical Society, New Series 63, 1-149.

Manzi G., Salvadei L., Passarello P., 1990. The Casal de' Pazzi archaic parietal: comparative analysis of a new fossil evidence from the late Middle Pleistocene of Rome. Journal of Human Evolution 19, 751-759.

Marra F., Ceruleo P., Pandolfi L., Petronio C., Rolfo M.F., Salari L., 2017. The aggradational successions of the Aniene River Valley in Rome: age constraints to early neanderthal presence in Europe. PLoS One 12, e0170434.

Marra F., Nomade S., Pereira A., Petronio C., Salari L., Sottili G., Bahan J.-J., Boschian G., Di Stefano G., Falguères C., Florindo F., Gaeta M., Giaccio F., Masotta M., 2018. A review of the geologic sections and the faunal assemblages of Aurelian Mammal Age of Latium (Italy) in the light of a new chronostratigraphic framework. Quaternary Science Reviews 181, 173-199.

Martínez-Navarro B., Madurell-Malapeira J., Ros-Montoya S., Espigares M.P., Medin T., Hortola P., Palmqvist P., 2015.

The Epivillafranchian and the arrival of pigs into Europe. Quaternary International 389, 131-138.

Martino R., Pandolfi L., 2022. The Quaternary *Hippopotamus* records from Italy. Historical Biology 34, 1146-1156.

Martino R., Ríos M. I., Mateus O., Pandolfi L., 2022. Taxonomy, chronology, and dispersal patterns of Western European Quaternary hippopotamuses: new insight from Portuguese fossil material. Quaternary International, https://doi.org/10.1016/j.quaint.2022.12.010.

Matsumoto H., 1924. Kinds of fossil elephaht from Japan (short report). Journal of Geological Society of Japan 31, 255-272.

Mazza P.P.A., 1991. Interrelation between Pleistocene hippopotami of Europe and Africa. Bollettino della Società Paleontologica Italiana 30, 153-186.

Mazza P.P.A., 1995. New evidence on the Pleistocene hippopotamuses of western Europe. Geologica Romana 31, 61-241.

Mazza P.P.A., Bertini A., 2013. Were Pleistocene hippopotamuses exposed to climate-driven body size changes? Boreas 42, 194-209.

Mecozzi B., Iurino D. A., Profico A., Rosa C. Sardella R., 2021. The wolf from the Middle Pleistocene site of Ostiense (Rome): The last occurrence of *Canis mosbachensis* (Canidae, Mammalia) in Italy. Historical Biology 33, 2031-2042.

Owen R., 1848. Description of teeth and portions of jaws of two extinct Anthracotherioid quadrupeds (*Hyopotamus uectianus* and *Hyop. bovinus*) discovered by the Marchioness of Hastings in the Eocene deposits on the N.W. coast of the Isle of Wight: with an attempt to develop Cuvier's idea of the classification of pachyderms by the number of their toes. Quarterly Journal of the Geological Society of London 4, 103-141.

Palombo M.R., 1986. Observations sur *Elephas antiquus* Falconer et Cautley du Pleistocène moyen d'Italie: essai d'évaluation des caractères dentaires. Geologica Romana 23, 99-110.

Palombo M.R., 2023. The Casal de Pazzi mammal fauna: Biochronological and paleoecological notes, and research perspectives. In: Gioia P., Milli S., Silvestri L. (Eds.), 40 Years of Casal dé Pazzi in the Framework of Pleistocene Archeo-Paleontological Sites (400.000-40.000 BP): Current Knowledge and New Research Perspectives. Journal of Mediterranean Earth Sciences 15, Special Issue, xx-xx.

Palombo M.R., Azanza B., Alberdi M.T., 2000-2002. Italian mammal biochronology from Latest Miocene to Middle Pleistocene: a multivariate approach. Geologica Romana 36, 335-368.

Palombo M.R, Ferretti M.P., 2005. Elephant fossil record from Italy: knowledge, problems, and perspectives. Quaternary International 126-128, 107-136.

Pandolfi L., 2013. Rhinocerotidae (Mammalia, Perissodactyla) from the Middle Pleistocene site of Ponte Milvio, Central Italy. Bollettino della Società Paleontologica Italiana 52, 219-229.

Pandolfi L., 2023. Reassessing the phylogeny of Quaternary Eurasian Rhinocerotidae. Journal of Quaternary Science 38, 291-294.

Pandolfi L., Bartolini-Lucenti S., Cirilli O., Bukhsianidze M., Lordkipanidze D., Rook L., 2021. Paleoecology, biochronology, and paleobiogeography of Eurasian Rhinocerotidae during the Early Pleistocene: The contribution of the fossil material from Dmanisi (Georgia, Southern Caucasus). Journal of Human Evolution 156, 103013.

Pandolfi L., Marra F., 2015. Rhinocerotidae (Mammalia, Perissodactyla) from the chrono-stratigraphically constrained Pleistocene deposits of the urban area of Rome (Central Italy). Geobios 48, 147-167.

Pandolfi L., Petronio C., Salari L., 2013. Catastrophic death assemblages from the Late Pleistocene of Italy: The case of Avetrana karst filling (Taranto, southern Italy). Rivista Italiana di Paleontologia e Stratigrafia 119, 109-124.

Petronio C., 1995. Note on the taxonomy of Pleistocene hippopotamuses. Ibex 3, 53-55.

Petronio C., Di Stefano G., Kotsakis T., Salari L., Marra F., Jicha B.R., 2019. Biochronological framework for the late Galerian and early-middle Aurelian mammal ages of peninsular Italy. Geobios 53, 35-50.

Quinn J.H., 1955. Miocene Equidae of the Texas Gulf Coastal Plain. Bureau of Economic Geology, The University of Texas, Publications 5516, pp. 102.

Sala B., 1986. *Bison schoetensacki* freud. From Isernia la Pineta (early mid-Pleistocene, Italy) and revision of the European species of *Bison*. Palaeontographia Italica 74, 113-170.

Sauqué V., Rabal-Garcés R., Madurell-Malaperia J., Gisbert M., Zamora S., de Torres T., Ortiz J. E., Cuenca-Bescós G., 2017. Pleistocene cave hyenas in the Iberian Peninsula: New insights from Los Aprendices cave (Moncayo, Zaragoza). Palaeontologia Electronica 20.1.11A, 1-38.

Segre A.G., 1983. Il giacimento preistorico di Rebibbia-Casal de' Pazzi (Roma). In: Beni Archeologici e valori ambientali in V Circoscrizione, Roma, 3-5.

Sher A.V., Garutt V.E., 1987. New data on the morphology of elephant molars. Transactions of the USSR Academy of Sciences. Earth Science Sections 285, 195-199.

Sotnikova M., 2010. Remains of Canidae from the lower Pleistocene site of Untermassfeld. In: Kahlke H.D. (Ed.), Das Pleistozän von Untermassfeld bei meiningen (Thüringen). 2. Habelt Verlag, Bonn, Germany, 607-632.

Tagliacozzo A., 2003. Archeozoologia dei livelli dell'Epigravettiano finale di Grotta Romanelli (Castro, Lecce) strategie di caccia ed economia di sussistenza. In: Fabri P., Ingravallo E., Mangia A. (Eds), Grotta Romanelli nel centenario della sua scoperta (1900-2000). Congedo Editore, Lecce, 169-216.

Zrzavý J., Duda P., Robovský J., Okřinová I., Pavelková Řičánková V., 2018. Phylogeny of the Caninae (Carnivora): Combining morphology, behaviour, genes and fossils. Zoologica Scripta 47, 373-389.